Using acoustic distortion products to measure the cochlear amplifier gain on the basilar membrane

J. B. Allen
Acoustics Research Department, AT&T Bell Laboratories, Murray Hill, New Jersey 07974-2070

P. F. Fahey
Department of Physics, University of Scranton, Scranton, Pennsylvania 18510-4672

(Received 8 November 1991; accepted for publication 26 March 1992)

Most models of the cochlea developed during the last decade have explained frequency selectivity and sensitivity of the cochlea at threshold by the use of power amplification of the acoustic wave on the basilar membrane. This power amplification has been referred to as the *cochlear amplifier* (CA). In this paper, a method to measure the cochlear amplifier gain as a function of position along the basilar membrane is derived from a simple model. Next, experimental evidence is presented that strongly restricts the properties of these proposed cochlear amplifier models. Specifically, it is shown that small signals generated by mechanical nonlinearities in the basilar membrane motion are not amplified during basilar membrane propagation, contrary to what would be expected from the cochlear amplifier hypotheses. This paper describes a method of measuring the cochlear power gain as a function of frequency and position, from the stapes to within 2 mm of the place corresponding to the frequency being measured. Experimental results in the cat indicate that the total gain of the cochlear amplifier, over the range of positions measured, must be less than 10 dB. The simplest interpretation of the experimental results is that there is no cochlear amplifier. The results suggest that the cochlea must achieve its frequency selectivity by some other means.

PACS numbers: 43.64.Kc, 43.64.Jb, 43.64.Bt

INTRODUCTION

For many years, researchers in the field of cochlear modeling have been struggling with the problem of cochlear tuning and cochlear sensitivity. By 1980 there was some acceptance of the idea that the basilar membrane (BM) may be functionally nonlinear, and several nonlinear models with level dependent BM damping had been introduced. Thus, when Kim *et al.* (1980a) introduced the idea of a negative damping, it seemed like a logical extension of previous work. In 1983 Davis (1983) wrote a nice summary paper where he coined the term *cochlear amplifier* (CA). Cochlear amplifier models were then further developed in greater detail by Neely and Kim (1986), and later by many others. Most recently Zweig (1991) has proposed a similar approach where propagated waves on the basilar membrane are amplified somewhat analogously to light waves in a laser. The common idea in cochlear amplifier models is that the basilar membrane impedance, over certain select regions of the cochlear, has negative damping. This gives rise to mechanical frequency selectivity similar to that of neural selectivity, and to a high sensitivity.

About the same time, it was observed that the cochlea produces spontaneous acoustic emissions that can be measured in the ear canal (Kemp, 1979). These emissions, called *spontaneous otoacoustic emissions* (SOAEs), were soon assumed to be byproducts of the proposed cochlear amplifier.

It is now widely accepted that the basilar membrane response is nonlinear, even at lower sound levels. This was first shown by Rhode (1971, 1978), and more recently by Sellick *et al.* (1982), and Robles (1986). It is believed that the function of the nonlinearity is to compress the large dynamic range of the acoustic signal at the ear drum to the much smaller dynamic range of the hair cell detectors. A byproduct of the nonlinear compression is the introduction of low-level mechanical and acoustical distortion products (DPs). Most recently it has been established that these distortion products are correlated to the threshold of hearing (Kemp, 1979; Kim *et al.*, 1980b; Fahey and Allen, 1985; Gaskill and Brown, 1990; Nelson and Kimberley, 1992; Leonard *et al.*, 1990; Probst *et al.*, 1991).

This paper reports on the use of distortion products to measure the power gain of the cochlear amplifier. A simple analysis that illustrates a method for measuring a spatially distributed cochlear amplifier gain is presented, with supporting experimental evidence from the cat, which fundamentally restrict these cochlear amplifier models. We present arguments, and experimental data, which show that the cochlear amplifier has a gain close to one. Furthermore, for frequencies between 0.8 and 8.0 kHz, our data are consistent with small middle ear power losses.

The basic idea is to use an acoustic distortion product, which is generated on the basilar membrane, as a source of acoustic energy. This is done while holding the magnitude of the response to the DP source constant at its characteristic

 0001-4966/92/070178-11$00.80

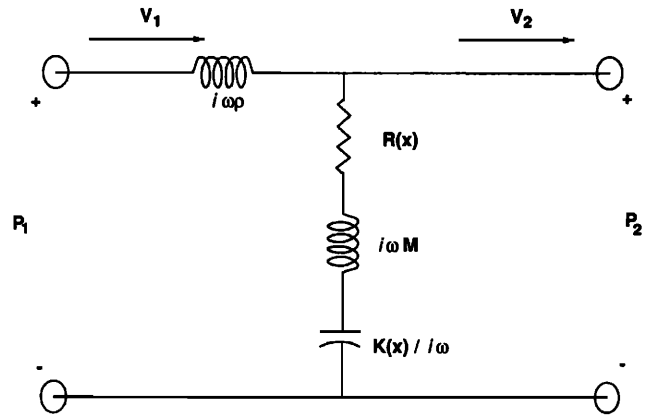

FIG. 1. Shown here is one section of a model cochlear transmission line. The cochlear fluid is treated as a series mass (element $i\omega\rho$), and the basilar membrane as a shunt impedance Z. The BM impedance consists of mass M, stiffness $K(x)$, and resistance $R(x)$. In the cochlear amplifier model, the resistance R is negative over some region of the BM. In these regions of negative R, the power must flow from the BM, rather than into it. The CA must be basal to the waves characteristic place for it to amplify the wave as it propagates.

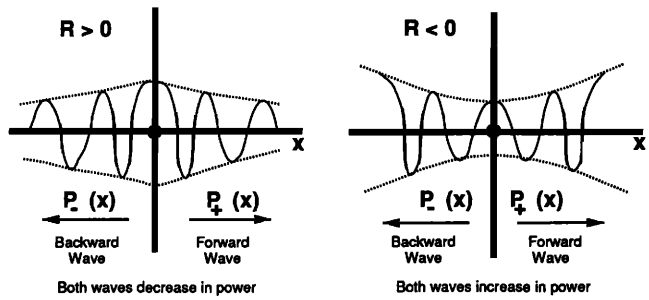

FIG. 2. We see here what happen to waves coming from a point source on the BM in regions of positive R, and negative R. In both cases, a forward and backward wave is generated. When the BM resistance R is positive ($R>0$), both waves decay in power. When the BM resistance is negative ($R<0$), both waves are amplified (the wave power increases).

place on the basilar membrane, by monitoring the rate response of a neuron tuned to the distortion product's frequency, while varying the location of the source on the basilar membrane. In our analysis, it is shown that as the source moves through a region of power gain, the distortion product pressure in the ear canal should vary as the *square* of the gain. Since the experimental results show no such systematic pressure variations, it is concluded that the basilar membrane power gain must be close to one.

I. WHAT IS THE COCHLEAR AMPLIFIER?

Since our goal is to measure the gain of the CA, its definition is necessary. The CA is best defined using the transmission line model of the cochlea, which is defined by the equations

$$\frac{\partial P}{\partial x} = -i\omega\rho V, \tag{1a}$$

$$\frac{\partial V}{\partial x} = -\frac{1}{Z}P, \tag{1b}$$

where x labels the position along the BM, $P(x,\omega)$ is the pressure across the basilar membrane, $V(x,\omega)$ is the basilar membrane velocity, ρ is the density of the cochlear fluid, and $Z(x,\omega) = K(x)/i\omega + R + i\omega M$ is the basilar membrane impedance. The BM stiffness is $K(x)$, the resistance is R, and the mass is M. In Fig. 1, we show the definitions in terms of a short section of the basilar membrane.

Equation (1) defines a second-order equation. This means that there must be two independent solutions, which may be characterized as a forward and a backward traveling wave. The properties of the two waves are best understood in terms of waves radiated by a point source located on the basilar membrane, as shown in Fig. 2. The local wave properties are determined by the impedances shown in Fig. 1. The phase, or wave velocity, is determined by impedances $K(x)$ and ρ, while the power flux (direction of wave power flow) is determined by the sign of resistance R. When R is positive, the waves are attenuated (the power flows into the basilar membrane). When R is negative, *both* waves are amplified.

We define the CA as a region on the basilar membrane where $R<0$. In general, the CA will depend on frequency. Since the forward wave must travel through the CA to be amplified,[1] the CA must be basal to its characteristic place. The assumed relation between the wave amplitude and the CA is shown in Fig. 3.

When a solution to the wave equation propagates, it does so with a *wave number* given by $\beta = \omega/c = 2\pi/\lambda$, where $\omega = 2\pi f$, λ is the wavelength, and c is the speed of the

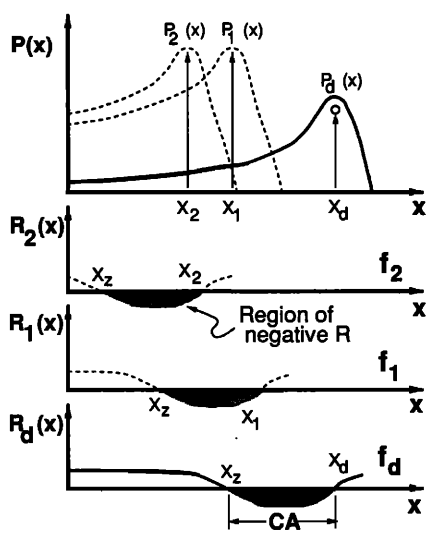

FIG. 3. In the top panel the pressure across the BM is shown at the three frequencies f_2, f_1, and f_d. This corresponds to a situation where two tones are played in the ear canal. The third tone, at f_d is the $2f_1 - f_2$ distortion product (DP) that results from nonlinear interactions of the primary tones on the basilar membrane. The DP is believed to be generated near the f_2 place x_2, because that is where the two primaries must have their maximum interaction. In the lower three panels, the assumed BM resistance is shown. Note how it is assumed to depend on frequency. We label the region of the CA to lie between $x_z(f)$ and the place of maximum response for a given tone.

wave. In this special case, the forward and backward wave solutions are proportional to

$$P^+(x) = e^{-i\beta x}, \tag{2a}$$

$$P^-(x) = e^{+i\beta x}. \tag{2b}$$

Unlike the case of the wave equation, the corresponding wave number for the cochlear equations of motion is a complex function of frequency and position. If we define this complex wave number γ by replacing $i\beta$ by $\gamma = \alpha + i\beta$, then $\alpha(x,\omega) > 0$ is a real positive function of frequency that accounts for the losses.

To account for power gain on the BM, one may change the sign of the loss term α, making the power loss negative. When α is positive, power is lost, regardless of the direction of the wave. When α is negative, the wave gains power, *again regardless of the direction of the wave.* Loss less ($\alpha = 0$) pressure gain, such as that found in a transformer, a loss less middle ear model, or in the pressure changes on the basilar membrane due to the longitudinal BM stiffness variations, are direction dependent. More important, such systems, *when terminated so that no reflections can occur,* have the property that if the magnitude of the pressure gain is G in one direction, it must be $1/G$ in the other direction (Carlin and Giordano, 1964, pp. 273, 330, and 315). This fact follows from energy conservation.

In summary, the important assumption made here is that when $R < 0$ the wave is amplified in a manner that is independent of its direction of propagation, as in the case of Eq. (1) described above.

II. THE EXPERIMENT

We propose to use the low-level nonlinear DP generator as a controlled source of energy on the basilar membrane. The signals are shown in Fig. 3. The ear canal signals are pressures p_1 and p_2 at frequencies f_1 and f_2, where $f_1 < f_2$. The primary frequencies are chosen such that the DP source at frequency $f_d = 2f_1 - f_2$ always has the same frequency, $f_1 = (f_2 + f_d)/2$, and f_2 is the independent variable. Furthermore, we maintain the amplitude of the DP traveling wave on the basilar membrane constant by monitoring its magnitude via a neuron tuned to f_d at location x_d on the basilar membrane. The pressure $P_d(x)$ across the basilar membrane at frequency f_d, and location x on the basilar membrane, represents a propagated distortion product. It is generally believed (but not proven) that P_d is generated near x_2, where $P_2(x)$ at frequency f_2 is maximum, because this is where the two primaries maximally interact on the nonlinear basilar membrane (Hall, 1974; Matthews and Molnar, 1986; Fahey and Allen, 1986).

At the DP frequency, the region of gain is believed to be distributed along the basilar membrane, basal to its characteristic place (Neely and Kim, 1986; Zweig, 1991), in the hatched regions of negative R of Fig. 3 labeled "←CA→." The source at x_2 may be moved along the basilar membrane by changing f_2. By varying p_2 and $p_1 = p_2$ in the ear canal, for each value of f_2, we may hold the DP pressure at place x_d at some fixed pressure $P_d(x_d) = P_0$ corresponding to the neuron's iso-rate condition. In Fig. 4, the source, and the resulting DP excitation pattern, is shown for two basilar membrane locations corresponding to a high frequency f_2 ($f_2/f_1 \to 2$) and a low frequency f_2 ($f_2/f_1 \to 1$). In the following, we assume that the CA has a total gain G.

From Fig. 4, when the source is near the stapes (f_2 high in frequency), the forward going wave is amplified by the CA gain G, and therefore the ear canal pressure must be $1/G$ *lower* than for the no-gain ($G = 1$) case. When the source is near x_d (low-frequency case), the backward traveling wave is amplified by the CA, and therefore the ear canal pressure is G *greater* than the no-gain case. Thus as the source is moved through the region of the CA, the ear canal pressure ratio must change by G^2.

In summary, by moving the DP source through the region of the CA (by changing f_2), while holding f_d and $P_d(x_d)$ constant (by monitoring the neutral rate of a unit at place x_d), we may infer the power gain of the CA as a function of x_2 from measurements of the change of the ear canal DP signal p_d. In the next sections, we formally derive this result, taking the reflection at the stapes into account. Readers not interested in this derivation may prefer to skip ahead to the "Experimental methods" section.

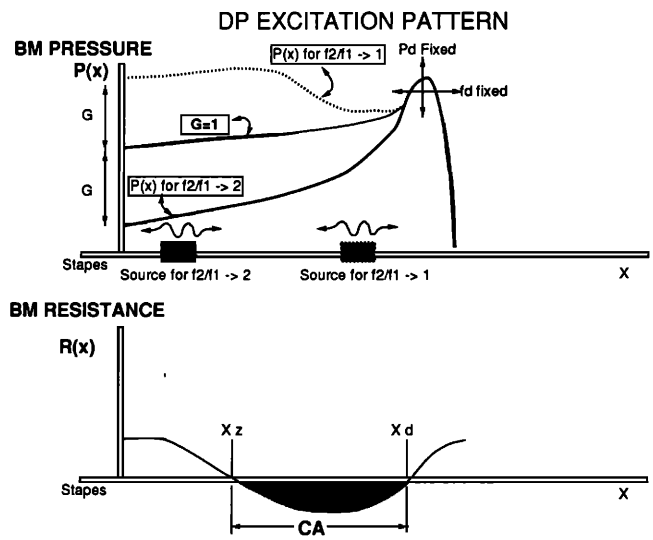

FIG. 4. This figure shows the traveling wave that must exist at the DP frequency f_d if the CA were present between x_z and x_d. The pressure $P_d(x_d)$ is held constant by measuring the rate of a neuron tuned to f_d at location x_d on the basilar membrane. Frequency f_d is held fixed, and primary frequency f_2 is varied, moving the source of the DP on the basilar membrane. When f_2 is high, the source is near the stapes (solid-bold line), and the wave is amplified as it propagates to x_d. Since the wave is assumed to be amplified by the CA gain G, and it is fixed in level at the neural observation point x_d, its level in the ear canal must be G dB lower than the case of no CA ($G = 1$, solid-thin line). As the primary frequency f_2 approaches the DP frequency f_d, and the source moves into the region of the BM gain, the ear canal pressure must approach a value of G dB greater than the no-CA case, because the reverse wave will be amplified by the CA. Thus, as f_2 is varied, the ear canal pressure at f_d should change by $2G$. If G is 40 dB, then we should see an 80-dB change!

III. DERIVATION OF THE CA GAIN

In this section, we outline the derivation of finding the CA gain $G(x)$ given the ear canal DP pressure $p_d(f_2)$ generated at x_2 and the neural frequency tuning curve $p_{\text{ref}}(f)$.

A. Definition of terms

A word about the notation is in order. Lower case p indicates pressure in the ear canal. We refer to the neural threshold tuning curve pressure in the ear canal as $p_{\text{ref}}(f)$. When $p_{\text{ref}}(f)$ is evaluated at f_d, we call the pressure p_0. Thus $p_0 = p_{\text{ref}}(f_d)$.

Upper case P indicates pressure in the cochlea. In all of the cochlear pressure equations (the upper case letters), the frequency is the distortion product frequency f_d. Assuming that the cochlea is modeled as a transmission line, then there must be two independent solutions P^+ and P^-. The forward pressure wave in the passive cochlea is P^+ and the retrograde pressure wave is P^-. The forward and backward waves depend on the source location, which is indicated by a second argument of $P^{\pm}$. Thus $P^+(x|x_2)$ is the pressure[2] for a forward cochlear wave at location x given a source of unit magnitude at x_2. The two waves are normalized so that $P^{\pm}(x_2|x_2) = 1$.

For example, for the special case of plane waves ($Z = K_0/i\omega$, $R = 0$, $M = 0$) with a source at x_2 and $x \geqslant x_2$,

$$P^+(x|x_2) = e^{-i(x-x_2)\omega/c}, \tag{3}$$

which represents a delay of $(x - x_2)/c$. The solutions $P^{\pm}$ of the cochlear equations, on the other hand, have a delay that is frequency and place dependent, with a sharp cutoff at the characteristic frequency (CF).

The *total* cochlear pressure P is the sum of the forward and retrograde wave. We shall call this total pressure $P_>(x|x_2)$ when $x > x_2$, and $P_<(x|x_2)$ when $x < x_2$, where the source is at x_2. We define the total cochlear pressure $P_>(x|0)$, with the source at the stapes ($x_2 = 0$), as the *reference* cochlear pressure $P_{\text{ref}}(x)$. The *neural-threshold* reference pressure at x_d is defined to be P_0. Thus $P_0 = P_{\text{ref}}(x_d) = P_>(x_d|0)$. Finally, the ratio of the total cochlear pressure at the stapes, with the source at x_2, to the total pressure at the stapes, with the source at the stapes is defined as $\Gamma = P_<(0|x_2)/P_{\text{ref}}(0) = P_<(0|x_2)/P_>(0|0)$.

We model the CA as a gain that modifies these passive waves. In general this gain will be a function of frequency and position. The gain may be specified either in dB per unit length, or as the gain (ratio of the pressures) at x for a source at x_2, $G(x|x_2)$. As in the case of the pressure, $G(x|x) = 1$. A source at x_2 radiates a wave in each direction. We call these radiated waves $G(x|x_2)P^+(x|x_2)$ and $G(x|x_2)P^-(x|x_2)$. We shall define the total gain from x_2 to x_d as G_+, and that from x_2 to the stapes as G_-. Thus

$$G_+(x_2) = G(x_d|x_2), \tag{4a}$$

$$G_-(x_2) = G(0|x_2). \tag{4b}$$

1. The middle ear assumption

In the following we assume that the ratio of any two pressures measured in the ear canal is equal to the ratio of two corresponding pressures behind the stapes in the vestibule. This means that we are treating the middle ear, in electrical terms, as a transformer, or in mechanical terms, as a lever. For example, suppose we have a source on the basilar membrane at x_2. We define p_2 to be the ear canal pressure, while $P_<(0|x_2)$ is the total scala pressure at the stapes. For the case where the source is at the eardrum, we define the ear canal pressure to be p_0 and the scala pressure at the stapes as $P_<(0|0)$. Thus our middle ear assumption is that

$$p_2/p_0 = P_<(0|x_2)/P_<(0|0), \tag{5}$$

namely the pressure ratio measured in the ear canal is the same as the pressure ratio measured at the stapes.

B. Predictions

We now develop a simple model that describes the pressure levels that we believe would be present in the ear canal at frequency f_d under the above conditions.

Two measurements are to be compared. Both measurements are at frequency f_d and are constrained so that the neural response is at threshold. The first is a *reference* condition, where the pressure in the ear canal is at the threshold pressure of the neuron. The second is the ear canal pressure which results from a DP source on the basilar membrane, generated near x_2. By comparing these two threshold measurements, the absolute neural threshold $P_0 = P_>(x_d|0)$ cancels. Basically, we calibrate a neuron by measuring its frequency tuning curve (FTC), which we call the reference condition. We then use this calibrated neuron as a detector to fix the pressure of the distortion product wave at the site of the neuron.

For the case of the DP source at x_2, we assume, with no loss of generality, that x_2 is *in* the region of power gain, with gain G_+ to the right, and G_- to the left. Thus the forward traveling wave is amplified by G_+ and the retrograde wave by G_-.

In modeling the general case of middle ear reflections, we divide the cochlea into two regions, $x > x_2$ and $x < x_2$. The *total* pressure in these two regions is defined as $P_>$ and $P_<$, respectively.

The pressure in the left-hand region $P_<(x|x_2)$ is the sum of a retrograde wave launched from x_2 and a forward traveling wave reflected from the stapes. The pressure $P_>(x|x_2)$ consists only of a forward traveling wave because no reflections are assumed in that region. Thus

$$P_>(x|x_2) = G(x|x_2)\,P^+(x|x_2)/A \tag{6}$$

and

$$P_<(x|x_2) = \frac{BG(x|0)P^+(x|0) + G(x|x_2)P^-(x|x_2)}{C}, \tag{7}$$

where A, B, and C are constants to be determined from the boundary conditions. Constant A is determined by the neural-threshold constraint at x_d, which is $P_>(x_d|x_2) = P_0$. Solving for A gives $A = G_+\,P^+(x_d|x_2)/P_0$. The reference condition is similar to Eq. (6), but corresponds to a pure tone excitation at frequency f_d at the stapes. The reference

condition pressure wave is $P_{\text{ref}}(x) = G(x|0)P^+(x|0)/A_{\text{ref}}$. The constant A_{ref} may be found from the neural boundary condition $P_{\text{ref}}(x_d) = P_0$, which gives $A_{\text{ref}} = GP^+(x_d|0)/P_0$.

The retrograde wave $P^-(x|x_2)$ is reflected from the stapes with a complex pressure reflection coefficient $\mathscr{R}$. At $x = 0$, B is found in terms of this reflection coefficient. The reflection coefficient is defined as the complex ratio of the reflected pressure to the incident pressure at the stapes. Setting the ratio of the two terms in the numerator of Eq. (7) equal to $\mathscr{R}$ results in $B = \mathscr{R}G_-P^-(0|x_2)$.

At x_2, C is found by matching the pressures in the two regions. Setting $P_>(x_2|x_2) = P_<(x_2|x_2)$, C is found, in terms of B and A, to be $C = A[1 + BG_-P^+(x_2|0)]$.

Thus all of the constants needed to evaluate $P_>(x|x_2)$ and $P_<(x|x_2)$, as given by Eqs. (6) and (7), and the reference condition $P_{\text{ref}}(x)$, have been determined.

1. Finding the relative ear canal pressure

The ratio of the stapes pressure due to a source at x_2 and that due to a source at the stapes is calculated next. The ratio $\Gamma = P_<(0|x_2)/P_{\text{ref}}(0)$ is, from Eq. (7) and the expression for P_{ref} given above,

$$\Gamma = \frac{A_{\text{ref}}}{A}\,\frac{G_-P^-(0|x_2) + B}{1 + BG_-P^+(x_2|0)}. \tag{8}$$

After some algebra this reduces to our final result, which is to be compared to the experimental measurements

$$\Gamma = G^2_-(1 + \mathscr{R}) \times \frac{P^+(x_d|0)P^-(0|x_2)}{P^+(x_d|x_2)\,[1 + \mathscr{R}G^2_-P^-(0|x_2)P^+(x_2|0)]}. \tag{9}$$

Invoking the middle ear assumption, Eq. (5), this ratio is equal to the corresponding ratio in the ear canal. Thus the variation of Γ with x_2 can be tested experimentally by ear canal measurements alone.

2. Case of no stapes reflections

If we evaluate the above expression for the special case of $\mathscr{R} = 0$, we find

$$\Gamma = G^2_-(x_2)\,\frac{P^+(x_d|0)P^-(0|x_2)}{P^+(x_d|x_2)}. \tag{10}$$

Thus for large f_2, $|\Gamma|$ will be close to 1, because by definition $G_- = 1$ when x_2 is at the stapes. As f_2/f_1 approaches 1, $|\Gamma|$ approaches G^2. The pressure terms in this expression correspond to the cochlear traveling wave delay and have only a small effect on $|\Gamma|$. Equation (10) may be solved for $G_-(x)$ in terms of Γ to give the gain. The pressure terms represent the cochlear latency.

3. Case of large gain

When $|\mathscr{R}G^2_-|$ is much greater than one, Eq. (9) reduces to

$$\Gamma = \frac{(1 + \mathscr{R})}{\mathscr{R}}\,\frac{P^+(x_d|0)}{P^+(x_d|x_2)P^+(x_2|0)}. \tag{11}$$

Thus when the gain is large, Γ is independent of the gain and is of order 1 in magnitude, and does not depend on G.

4. Case of intermediate gain

When the frequency f_2 is high, G_- must start at 1 because x_2 is at the stapes. As the frequency f_2 is reduced, the gain increases, and for some f_2 $|\mathscr{R}G^2_-| = 1$. Depending on round trip phase delay between x_2 and the stapes, as determined by $P^-(0|x_2)P^+(x_2|0)$, the denominator of Eq. (9) can go to zero, causing Γ to become arbitrarily large.

When this condition occurs, the amplified wave reflected from the stapes cancels the forward wave originating from x_2. In order to satisfy the neural boundary condition, the primary tones are then increased in an attempt to keep the neuron at threshold. Depending on the accuracy of the cancellation, this will require arbitrarily large primary levels. By changing the acoustic impedance in the ear canal, it is possible to change $\mathscr{R}$ in either magnitude or phase, which could be an important experimental degree of freedom near the $|\mathscr{R}G^2_-| = 1$ point.

If there were no CA, then $|\mathscr{R}G^2_-|$ will always be less than 1, and poles in Γ cannot occur.

5. Case of nonlinear gain

The primary levels are typically 30 to 40 dB greater than the DP levels. This opens the possibility that the CA gain may be suppressed by the primary signals when $f_2/f_1 \to 1$. Referring again to Fig. 4 we can see what will happen in this case. For the high frequency f_2, the primaries will be far from the CA, and will therefore not suppress the CA gain. Thus the wave will be amplified by the CA gain G, as before. However, if we assume that for the low-frequency case, that the gain is totally suppressed by the primaries, then the reverse traveling wave will not be amplified, because the CA gain will be 1. In this case, the ear canal pressure difference, as a function of f_2, will be G rather than G^2. If the gain were suppressed to a value of G_1, then the total pressure change would be GG_1, rather than G^2. This means that we would be able to measure the gain change as a function of the degree of suppression, which would make the results very interesting indeed.

IV. EXPERIMENTAL METHODS

The preparation was previously described (Fahey and Allen, 1985; Allen, 1983). Young adult cats were prepared for neural recording using the dorsal approach. The cerebellum was retracted and the internal auditory meatus and cochlear nerve exposed. An earphone was placed in the animal's ear canal and was calibrated using a small probe microphone that was also in the canal. The microphone probe tube was typically about 3 to 4 mm from the umbo. The transducer was designed to have a source impedance that was close to that of the ear canal. Thus the transducer reflection coefficient $\mathscr{R}$ was small, and was about 0.2–0.3 over

most of the frequency range. For more information on the impedance of the transducer see Allen (1985).

A microelectrode was then advanced into the auditory nerve while gated noise was presented to the ear canal. The noise served as a search stimulus. Once an auditory neuron was acquired, the frequency tuning curve (FTC) $p_{\text{ref}}(f)$ was measured, using the FTC paradigm of Moxon and Kiang (Allen, 1983).

A. DP generation

Next the DP experiment was run using a modified FTC paradigm. Based on the FTC, frequency f_d was chosen, thereby fixing the reference pressure $p_0 = p_{\text{ref}}(f_d)$. Two tones served as the stimulus, $p_1(f_1)$ and $p_2(f_2)$. We began with p_2 and f_2 at their maximum possible values for the transducer. These were close to 80 dB for p_2 and 30 kHz for f_2. The lower frequency f_1 was computed from the formula $f_1 = (f_2 + f_d)/2$, where f_d is the best frequency of the neuron's response. The computer feedback loop then adjusted the levels of p_1 and p_2, which were always held equal for these experiments, until the neuron was responding at one spike/50 ms greater than its spontaneous rate. The tones were gated on and off with a 50-ms duration and a 50-ms silence. Spikes were counted during the two intervals and compared. The procedures are described in Fahey and Allen (1985).

Once the threshold level was obtained (or if the distortion product was insufficient to drive the neuron), f_2 was decremented and the procedure was restarted. The levels of the ear canal primaries and the DP were recorded at the neuron's threshold level. These levels were displayed, along with the tuning curve of the unit, as the data was collected. We refer to this condition as the *closed-loop* condition.

Frequently, as a control, the neural signal was disconnected from the computer, opening the feedback loop. In this case, the computer presented the maximum level signals to the ear canal, and the unit responded to the DP with super-threshold levels. These results were also displayed. We refer to any condition where the DP level was not actually held at the neuron's threshold level P_0 as the *open-loop* condition. For example, if the primary level resulted in a DP that was below the threshold of the neuron, the primary pressure was limited to the maximum pressure and the condition is referred to as an open-loop condition. The frequency decrement was large (10 points per decade) for open-loop conditions and small (40 points per decade) for the closed-loop conditions.

A second control was also run where we reduced the primary level by 40 or more dB. This allowed us to measure the DP noise floor at f_d. We called this the *attenuated* condition.

We have made these DP measurements on 227 neurons having normal CF thresholds and tuning characteristics which ranged from 0.7–10 kHz, across 9 animals. For about 10% of the neurons we ran both controls (the open-loop and attenuated conditions), which independently demonstrated for these cases that (a) the maximum possible DP level was greater than the CF threshold, and (b) the noise floor at f_d was below the DP level. These are the conditions necessary for an artifact-free closed-loop region. For about 50% of the remaining neurons, the ear canal DP level and the tuning curve were measured, but the two controls were not measured. In these neurons we do not know the maximum level of the DP. Thus we do not have an independent check on the close loop frequency interval or an independent check on the noise floor. The remaining neurons (about 40%) provided little data for a number of reasons, such as loss of neural recording, noise during the recording, poor recording conditions, etc.

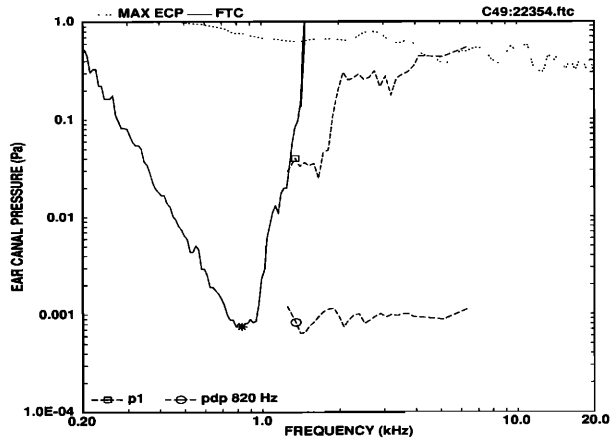

FIG. 5. The solid line shows the neural tuning curve (FTC). The DP is placed at the CF (f_d = 820 Hz). The higher frequency primary frequency f_2 is swept from high to low frequency, with $f_1 = (f + f_d)/2$. The maximum possible ear canal primary pressure (MAX ECP) is shown by the dotted line at the top. Each measurement is shown as a pair of curves. The curve labeled with a □ is p_1 (f_1), while the curve labeled with a O is the DP pressure $p_d(f_1)$. The DP pressure is plotted as a function of f_1 even though it is at f_d, so that we can observe how it changes as f_2 is varied. The pressures p_2 and p_1 were always equal. Pressure p_2 is not shown. All pressures are measured in the ear canal.

V. RESULTS

The solid line in each of the Figs. 5–8 shows $p_{\text{ref}}(f)$, the frequency tuning curve for the neuron. The tight-dotted line at the top of each figure shows the maximum primary tone pressure that may be delivered by the transducer. The primary levels were always equal. The abscissa is in kHz, and the ordinate is in Pascals (one Pascal is 94 dB SPL). All displayed pressures are measured in the ear canal. For each frequency sweep, two pressures are plotted, $p_1(f_1)$, the ear canal pressure of the lower frequency primary, and $p_d(f_1)$, the ear canal distortion product pressure. The DP pressure p_d is always plotted as a function of the lower primary frequency f_1 so the points may be distinguished. We plot p_1 rather than p_2 so we may see when the neuron begin responding to the primary rather than the DP. This pair of corresponding pressure curves are plotted using the same dashed line type. The primary pressure p_1 is labeled with a □ and the DP pressure is labeled with a O. The reference pressure p_0, at frequency f_d, is indicated by a * on the tuning curve.

Typical results are shown in Figs. 5 and 6. Initially, for very high f_2, the two tones are far apart and the DP on the BM is too small to excite the neuron (the open-loop condi-

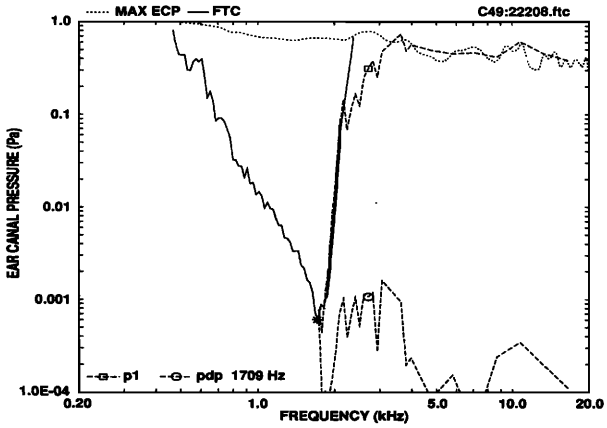

FIG. 6. The solid line is the tuning curve of the neuron being measured. The best frequency of the neuron is 1.709 kHz. The short-dashed line at the top of the figure shows the maximum ear canal primary pressure that may be delivered to the ear canal, corresponding to 3.5 V to the earphone. The ordinate is the ear canal pressure. One Pascal (PA) is 1 Nt/m^2, which corresponds to 94 dB SPL. The upper dashed line shows the pressure of the lower frequency primary p_1 as a function of f_1. The lower dashed line shows the ear canal distortion product pressure p_d at frequency $f_d = 1709$ Hz, also plotted as a function of f_1.

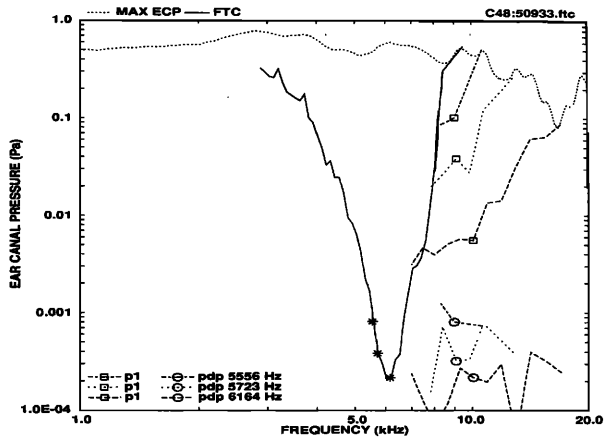

FIG. 8. In this figure, we varied the reference pressure by changing the frequency of the DP. In this way we manipulated the magnitude of the DP on the BM. We have removed the data outside of the closed-loop region for clarity.

tion). However as f_2 is reduced, the two tones move closer in frequency, and the magnitude of the DP increases. At 4.0 kHz, Fig. 5, the propagated DP begins to excite the neuron, and the computer begins to lower the primary levels, reducing the spike rate to threshold (the closed-loop condition). As f_2 is lowered further, the level of p_1 and p_2 continue to drop. When p_1 intersects the tuning curve (at 0.04 Pa and 1.2 kHz for Fig. 5), $p_1(f_1)$ begins to excite the neuron directly,

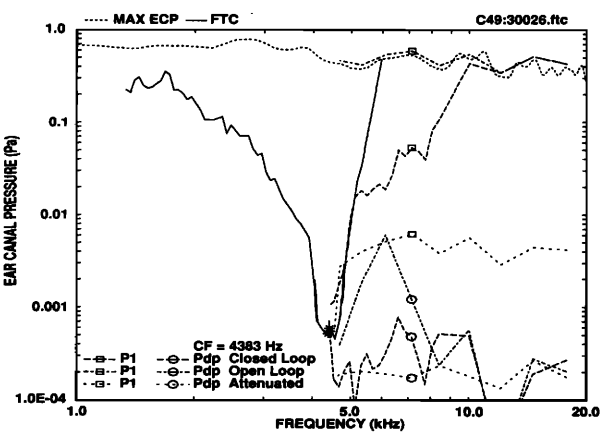

FIG. 7. This figure shows similar results to those of Figs. 5 and 6, however, in this case, two controls have been run. In one case (wide-spaced dashed line with symbol □) the signal to the ear canal has been attenuated by 40 dB. This caused the corresponding DP pressure (same line type, but at bottom) to drop to the acoustic noise floor. In the second control, dash-dot line, the neural response was disconnected from the computer, causing the full signal (about 80 dB SPL) to go to the canal. This caused the DP in the ear canal (lower dash-dot line with symbol O) to increase dramatically. It peaked at about 6 kHz in this case. These two controls show the limits of the DP signals in the ear canal.

and the sweep is complete. The lower dashed curve labeled with a O shows $p_d(f_1)$ for this unit. Over the closed loop-region from 1.2–4.0 kHz, the DP pressure remains close to 0.001 Pa (34 dB SPL).

In Fig. 6 we see a similar pattern. For frequencies between 3.8 and 20 kHz, the DP is too small to drive the neuron. For frequencies between about 2.05 kHz and the CF at 1.709 kHz, the neuron is driven by the f_1 primary. Between 2.05–3.8 kHz, the neuron is driven by the DP in the closed-loop condition. Over this frequency range the primary level drops from the maximum to about 0.1 Pa. It has a 6-dB oscillation as it drops. The DP level remains constant, on the average, but has 10-dB periodic fluctuations with a frequency spacing between 100 and 200 Hz.

These variations have several possible sources. First are standing waves due to reflections at the stapes and middle ear. Second is the inherent variability due to the tuning curve search procedure. Third is that the source is distributed over a small region on the basilar membrane, leading to possible interference effects between neighboring components.

We conclude three things from these and other data like them. *First*, based on the periodic nature of the fluctuations, the most likely explanation for the fluctuations is standing waves between the stapes and the site of DP generation. Only standing waves can explain the quasiperiodic nature of the variations. A distributed source of distortion would give a more random pattern with less frequency (fewer) nulls. The density of the data samples was insufficient in most cases to adequately resolve the standing waves. (If we were to repeat the experiment, this resolution would be increased.)

Second, the gain of the cochlear amplifier must be close to one. Over the closed-loop range, the maximum DP level stays within a 3- to 10-dB range. This would imply, based on Eq. (9), a power gain between ± 5 dB. From the extended data base, we noticed that as f_2 decreases, p_d tends to slightly (e.g., 6 dB) decrease. If the organ of Corti generated signal power, the maximum ear canal DP should increase rather

than decrease as f_1 and f_2 approach f_d.

Third, the DP traveling wave is tightly coupled to the ear canal. It is clear from these two examples, that in the close-loop region, the peak value of the ear canal DP pressure is very close to the neuron's threshold pressure (Fahey and Allen, 1985). From Eq. (10), this can only happen if $G_-(f_2)$ is close to one. The passive pressure gain of the middle ear (due to the ratio of the eardrum to stapes footplate area) and the basilar membrane (due to the stiffness variation along the BM) both cancel in this comparison. The passive (loss less) pressure gain produced by the middle ear in measuring the tuning curve at f_d compensates the passive pressure gain of the middle ear for the DP that is reverse propagated. Middle ear power losses, on the other hand, do not cancel. (In data not shown, power losses *were* found below 800 Hz, which increased with decreasing DP frequency.)

A third example is given in Fig. 7. In this figure we show results for the closed-loop condition, the open-loop condition, and the attenuated condition. The closed-loop condition ranges over f_1 values from 5.0 to 10.0 kHz and the DP varies from 1×10^{-4} to 0.8×10^{-3} Pa. For f_1 between 6.0 and 10 kHz, the DP stays within an 8-dB range except for a dip 7.8 kHz. This 8-dB range is centered on 0.0005 Pa (28 dB SPL), which is within a few dB of p_0 (indicated by the *).

The open-loop condition gave an ear canal DP that peaked at $f_1 = 6.0$ kHz. This corresponds to an f_2/f_1 of 1.3. This ratio is typical for the cat for f_2 values of 7.8 kHz (Fahey and Allen, 1985, Fig. 1, p. 317). Since the frequency steps used during the open-loop condition were larger than those used during the closed-loop, the frequency where the DP peaked was not accurately determined. Note that the maximum occurs well before f_1 intersects the tuning curve.

The attenuated condition was measured with an attenuator setting of 40 dB. This gave a primary level close to 0.004 Pa. The associated noise floor in the ear canal at f_d was at 2×10^{-4} Pa (20 dB SPL). This shows that the noise floor at f_d was at least 10 dB below the maximum DP level during the closed-loop measurement (f_1 between 5 and 10 kHz).

In a fourth example, shown in Fig. 8, we varied f_d slightly so that the reference sensitivity p_0 changed. Three different pressures were tried, as defined by the three *'s on the tuning curve $p_{\text{ref}}(f)$. In each case the DP amplitude $p_d(f_1)$ was approximately equal to p_0 within the closed-loop region of the frequency sweep. Increasing p_0 required larger primaries, and therefore the frequency range of the closed-loop region decreased. The ratio of the change in the primary level to the DP level lies between 2 and 3, with the larger ratio at lower levels. A 12-dB change in the DP level corresponds to a 26-dB change in the primary level. This gives an average compression ratio of about 2 to 1.

The results of Fig. 8 show that our conclusions are not limited to, or dependent on, a particular level of the primary pressure. The lowest primary level is about 45 dB SPL (long-dashed line labeled 6164 Hz). The corresponding p_0 at the neural CF threshold is about 20 dB SPL. Thus the difference between the primary and the distortion product level is about 25 dB. It is hard to reconcile these data at these low sound-pressure levels with models having a nonlinear CA saturation, such as those that might be required when modeling two-tone suppression.

VI. DISCUSSION

For DP frequencies above 1 kHz, the DP amplitude in the ear canal was found to be approximately equal to the reference threshold of the neuron. In other words, regardless of whether the source is in the canal (delivered by a transducer) or on the basilar membrane (due to the nonlinear generator), the pressure in the ear canal at the source frequency remains approximately the same, as long as the neural rate at f_d is held constant. We interpret this observation to mean that any power losses or gains in the cochlea and middle ear are small. The simplest interpretation of our experimental results is that there is no cochlear amplifier. The results suggest that the cochlea must achieve its selectivity by some other means.

In none of our data was there convincing evidence for cochlear power gain. Conservatively expressed, our results are consistent with a power gain that is less than 10 dB (a closed-loop variation of less than 20 dB). In fact, some of our data showed a small power *loss* near the CF rather than a gain (e.g., Fig. 7), in that the DP amplitude in the closed-loop region decreased slightly as f_2 approached f_d. This effect, if real, was too small to quantify. We view this as an indication of cochlear losses near the CF due to damping within the organ of Corti. If the cochlea had a power gain, then the DP pressure should increase rather than decrease. In passive cochlear models, the impedance basal to the characteristic place is stiffness dominated, with a stiffness that increases as x_2 moves toward the base. If follows that there must be very small losses basal to the characteristic place. In these models, a tone burst in the ear canal is propagated along the cochlea *without significant power loss* until it approaches its characteristic place. In CA models, the tone burst is amplified as it propagates.

Models for cochlear amplifiers (e.g., Neely and Kim, 1986; Zweig, 1991) find it necessary to place the cochlear gain basal to the best frequency. This makes sense, since the CA must be basal to the CF if the wave is to be amplified as it propagates to the CF. For these models, we feel that our experimental results represent a severe constraint. That is, if there is a CA, then it must be localized to within 1 mm of the CF. Based on excitation patterns derived from neural tuning curves, we believe that any active region should begin 2–3 mm from the CF, for a CF of 1 kHz (as will be discussed below).

Our interpretation has assumed isotropic BM wave propagation. We believe that the isotropic assumption is realistic, and that the traveling wave on the basilar membrane will be isotropic. We raise this issue only because it is an important assumption of our analysis. All the models (active and passive) have isotropic wave propagation. The Zweig model also assumes isotropic basilar membrane wave propagation, but uses a time delayed feedback to realize the amplifier. Is this proposed feedback delay in the class of isotropic propagation? Zweig's "laser" analogy suggests that amplification occurs symmetrically. If in the Zweig model, propa-

gation were nonisotropic, then that model is also constrained by our experimental results. However, in that case, our model will not accurately predict this constraint.

We know that the middle ear reverse transfer function depends on the load impedance of the earphone and ear canal on the eardrum impedance (impedance of the ossicle and cochlear input impedance). For example, if the earphone impedance were equal to the eardrum input impedance, then the attenuation of the DP should be 6 dB. This was approximately the situation for our measurements. This loading effect may be compensated for, if the earphone impedance and the eardrum impedance are known (Fahey and Allen, 1986).

A. Two-tone suppression and the CA

We next explore the effect that two-tone rate suppression might have on our results. The concern is that as the higher frequency f_1 primary approaches f_d, the neural sensitivity p_0 will change due to the rate suppression effect (Fahey and Allen, 1985). Thus the CA would be compensated by the decreased sensitivity of the rate-suppressed neuron. Could it be that there is a relation between the two-tone suppression and the CA such that the product of the two is always constant, thereby giving a constant ear canal pressure?

There are three ways we have approached this question. The first relates back to the discussion of Fig. 4 where we observed that if the primary were to suppress the CA gain for the low frequency f_1, then the resulting gain change would be G rather than G^2. Since we did not see any increase in the DP pressure, we may still conclude that there is no CA, even though it could have been suppressed by the high level primary.

The second argument is based on the results of Fig. 8 where we have changed the primary level by 30–50 dB, and the result (namely, $p_d = p_0$) does not change. The fact that $|\Gamma|$ is *independent* of primary level strongly argues against a two-tone suppression interaction with the CA.

Finally, we have limited direct experimental evidence that suppression probably does not affect our conclusions. In a small number of the neurons studied, suppression thresholds were measured after Fahey and Allen (1985). Almost without exception, both the lower and the higher frequency primary tones, under the closed-loop conditions, were well out of the area of suppression for these units.

B. Estimating the region of the CA

Since we have assumed that the DP source is in the region of the CA, it is important to try to independently estimate this region on the basilar membrane. One approach would be to look at the CA regions assumed in the models. It is difficult to identify these regions from published information. Alternatively, we attempt to estimate the CA region directly from neural excitation patterns. The derivations of these curves, detailed in Allen (1990), is based on neural tuning curve data from the cat.

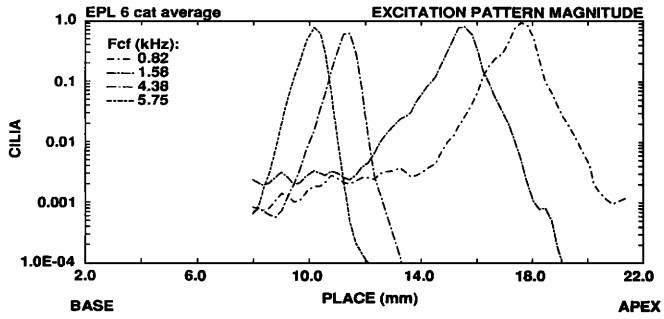

FIG. 9. Shown here are four neural excitation patterns derived from families of neural tuning curves. The exact procedure is described by Allen (1990). Excitation patterns show the neural response as a function of place x for a given frequency while neural tuning curves show the neural response as a function of frequency for a given place. The four frequencies that have been chosen correspond to f_d and f_2 of Figs. 5 and 7. For a frequency of 1.58 kHz, the response maximum (CF) is about 15.5 mm. The 1.58-kHz excitation pattern shows a break in slope near 11.5 mm. For the 4.38-kHz excitation pattern, the break in slope is near 9 mm. We have defined this frequency dependent break point as $x_z(f)$, and plotted it as a dashed line in Fig. 10. We assume that the cochlear amplifier must exist between x_z and x_{CF}, because x_z is where the response increases. To the left x_z is the "tail" region of the tuning curve, and to the right is the "tip" region. By extrapolating the tail to x_{CF}, and measuring the pressure difference to the tip, we attempt to estimate the gain of the CA. This estimate assumes that the change in slope at x_z is due to the CA. The total magnitude of the increase is about 40 dB. The CA is believed to have a gain of about 40 dB (A pressure gain of 100, or a power gain of 10 000).

If the basilar membrane resistance were to become negative at some point, changing the damping to a power gain, then one would expect to see a change in the excitation pattern *slope* at that point. In Fig. 9, we show four excitation patterns corresponding to frequencies 0.82, 1.58, 4.38, and 5.75 kHz. We pick these frequencies because they correspond to the f_d and f_2 of Fig. 5 and Fig. 7. From the excitation patterns one may see a basal "tail" region, and a region where the response starts to build, having a steeper slope. We define the location where the slope increases x_z. For a 1.58-kHz tone, x_z occurs near 11.5 mm, while the characteristic place is at 15.5 mm. For the 4.38-kHz excitation pattern, x_z is at 8.9 mm, while the characteristic place is at 11.2 mm. In Fig. 10, we have plotted both $x_z(f)$ and $x_{CF}(f)$ as a function of the tone frequency based on many such excitation patterns.[3] If we interpret the point $x_z(f)$ as the point where the CA begins, then the CA would lie between the two curves of Fig. 10. A figure similar to this one is given in Allen (1980), Fig. 2.

To estimate the gain G_- of the CA corresponding to the experimental condition of Fig. 5, we look at the excitation patterns (EPs) corresponding to $f_d = 0.820$ kHz and $f_2 = 1.58$ kHz. We would like the gain at x_2 for frequency f_d. If we look at the f_d excitation pattern at $x_2 = 15.5$ mm, we may see how much it has increased over the level in the tail region. At 14 mm, where the slope of the EP changes, the 0.82-kHz excitation pattern has a relative level of 0.003, while at 15.5 mm, the x_2 place, it is 0.02 mm. This gives a gain of 0.02/0.003, or 16.48 dB. The same calculation for the data of Fig. 7 gives 28 dB, and for Fig. 8 with $f_d = 6.164$ and

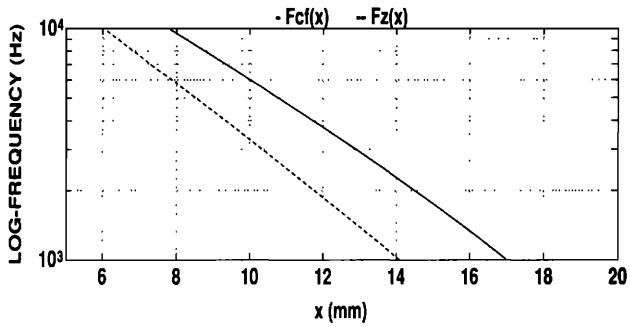

FIG. 10. Shown here is the cochlear map of the cat (solid line) and a second cochlear map that corresponds to the place on the excitation pattern where the slope changes. We call this place $x_z(f)$. We have plotted the inverse of the function $F_z(x)$. For example, in Fig. 9 for the 0.82-kHz excitation pattern, the CF is at 17.5 mm and x_z is at 14.5 mm. For the 4.38-kHz excitation pattern, x_z is at 9 mm.

$f_2 = 7.84$ kHz, $G_- = 30$ dB. If we were to assume that the DP were generated at the $(f_1 f_2)^{1/2}$ place rather than at the f_2 place, then these estimated gains would be significantly larger.

We conclude that x_2 must have extended far enough into the CA region to observe a measurable gain change. Since the DP pressure is constant (there is no CA), we conclude that the change in slope at $x_z(f)$ seen in the excitation patterns is *not* due to a CA, and it must be accounted for by another physical mechanism (Allen, 1990).

C. Spontaneous emissions

If the CA hypothesis is false, how can the cochlea emit spontaneous emissions? This question is difficult to answer because we know so little about how SOAEs are generated. First, no one has shown that SOAEs *must be* due to an active mechanism. And if they *were* due to an active mechanism, it is not clear why or how the CA would be involved in the generation process. In fact, one can argue that if there were a CA, then the SOAEs would have very different properties. For example, the CA will not generate SOAEs unless it is terminated with reflecting boundaries, causing waves to travel back and forth through the CA. This would mean that the wave would be amplified by G on each trip. If G were as large as is required by the CA used in models (e.g., 40 dB), the SOAEs would be huge after a few round trips.

In fact, standing waves do seem to be a reasonable explanation for the SOAEs for several reasons, but with a gain for G of 1. The standing wave model was first described by Kemp (1979). In that model, low level noise, such as thermal noise, is reflected back and forth between its place on the BM and the plugged ear canal. Just as for standing waves in a pipe, the thermal noise floor would be passively amplified to give peaks that would be observed as emissions. A very important property of SOAEs is their multiplicity. They come in groups, with a frequency spacing of approximately 90 Hz. The exact frequency spacing depends on frequency. The delay between the stapes and $x_d(f)$ seems to account for this component spacing. If the reflection coefficient at x_d at threshold levels were nonlinear, with the reflection coefficient decreasing for higher signal levels, then the amplitude distribution would be non-Gaussian, as has been reported by Bialek and Wit (1984). A non-Gaussian distribution does not require an active system. Given a nonlinear reflection coefficient, it is possible to have a non-Gaussian amplitude distribution given a Gaussian input. In fact, if the reflection coefficient were a zero-memory nonlinear system described by $y = g(x)$, driven by a signal x with probability density function $p(x)$, then the output will have probability density function $p(y)$ with $p(y) = p(x)/(|dy/dx|)$ (Bendat, 1990, p. 25). This discussion leaves unexplained the very high-level emissions that have been observed in a small number of cases (for a discussion of this point see Probst *et al.*, 1991).

D. Standing waves versus SOAEs

If there are standing waves in the ear, such as those observed in Fig. 5, then why don't we see emissions in our measurements? First, emissions are not typically seen in the cat. Second, the transducer that we used in these experiments is approximately matched to the impedance of the ear canal of the cat; thus reflections in the ear canal, when using this transducer, are greatly reduced. Furthermore we believe the coupling between the ear canal and the cochlea, between 1–3 kHz, to be close to one. This is known from reflection coefficient measurements in the ear canal (made at high levels), which are less than 0.1 for these frequencies (Puria and Allen, 1991). It is also supported by the results reported on here. Most ear canal experiments do not use a matched transducer, but seal the transducer in the canal with a foam or hard rubber plug. For animals where spontaneous emissions are measured, the ear canal reflection coefficient at the cochlea-stapes boundary could easily be between 0.8 and 1.0 for frequencies near 1 kHz due to the unmatched ear canal transducer.

If the experiment done here in cat were to be repeated in an animal having SOAEs, this would clarify the relation between the CA and SOAEs. If in these animals the gain of the cochlear amplifier were also close to one, then perhaps it would be time to reevaluate some of the ideas from the 1970s such as the "second filter," approach of Evans and Wilson, and reexamine the implication of the pressure measurements of Dancer and Frank (1980), and the propagated DP phase measurements of Kim *et al.* (1980b). These experimental results have been largely ignored, since they were inconsistent with aspects of the CA hypothesis. If the CA hypothesis is false, then we need to again explore alternative explanations of how the cochlea works.

ACKNOWLEDGMENTS

We would like to thank Chris Shera, Sunil Puria, George Zweig, and reviewer Rich Schmiedt, for their helpful comments and constructive criticisms.

[1]We define the forward wave as that traveling from the stapes, in the base, toward the apex.

[2]The vertical bar should be read as "given;" thus $P(y|x)$ is "the pressure at location y given a source at location x."

[3]Actually we have plotted the inverses of these functions $F_z(x)$ and $F_{CF}(x)$.

Allen, J. B. (**1979**). "Cochlear models—1979," in *Models of the auditory system and related signal processing techniques*, edited by M. Hoke and E. DeBoer, Scand. Audiol. Suppl. 9, 1–16.

Allen, J. B. (**1980**). "Cochlear micromechanics—A physical model of transduction," J. Acoust. Soc. Am. **68**, 1660–1670.

Allen, J. B. (**1983**). "Magnitude and phase frequency response to single tones in the auditory nerve," J. Acoust. Soc. Am. **73**, 2071–2092.

Allen, J. B. (**1985**). "Measurement of eardrum acoustic impedance," in *Peripheral Auditory Mechanisms*, edited by J. B. Allen, J. L. Hall, A. Hubbard, S. T. Neely, and A. Tubis (Springer-Verlag, New York), pp. 44–51.

Allen, J. B. (**1990**). "Modeling the noise damaged ear," in *The Mechanics and Biophysics of Hearing*, edited by P. Dallos, C. D. Geisler, J. W. Matthews, M. A. Ruggero, and C. R. Steele (Springer-Verlag, New York), pp. 324–332.

Bendat, J. S. (**1990**). *Nonlinear system analysis and identification from random data* (Wiley, New York), p. 25.

Bialek, W., and Wit, H. P. (**1984**). "Quantum limits to oscillator stability: Theory and experiments on acoustic emissions from the human ear," Phys. Lett. **104A**, 3, 173–178.

Carlin, H. J., and Giordano, A. B. (**1964**). *Network Theory, An Introduction to Reciprocal and Nonreciprocal Circuits* (Prentice-Hall, Englewood Cliffs, NJ), pp. 273, 315, and 330.

Dancer, A. L. and Frank, R. B. (**1980**). "Intracochlear sound pressure measurements in guinea pigs," Hear. Res. **2**, 191–205.

Davis, H. (**1983**). "An active process in cochlear mechanics," Hear. Res. **9**, 1–49.

Fahey, P. F., and Allen, J. B. (**1985**). "Nonlinear phenomena as observed in the ear canal and at the auditory nerve," J. Acoust. Soc. Am. **77**, 599–612.

Fahey, P. F., and Allen, J. B. (**1986**). "Characterization of cubic intermodulation distortion products in the cat external auditory meatus," in *Peripheral Auditory Mechanisms*, edited by J. B. Allen, J. L. Hall, A. Hubbard, S. T. Neely, and A. Tubis (Springer-Verlag, New York), pp. 314–321.

Gaskill, S. A., and Brown, A. M. (**1990**). "The behavior of the acoustic distortion product, $2f_1 - f_2$, from the human ear and its relation to auditory sensitivity," J. Acoust. Soc. Am. **88**, 821–839.

Hall, J. L. (**1974**). "Two-tone distortion products in a nonlinear model of the basilar membrane," J. Acoust. Soc. Am. **56**, 1818–1828.

Kemp, D. T. (**1979**). "Evidence of mechanical nonlinearity and frequency selective wave amplification in the cochlea," Arch. Otorhinolaryngol. **224**, 37–45.

Kim, D. O., Neely, S. T., Molnar, C. E., and Matthews, J. W. (**1980a**). "An active cochlear model with negative damping in the cochlear partition: Comparison with Rhode's ante- and post-mortem results," in *Psychological, Physiological, and Behavioral Studies in Hearing*, edited by G. van den Brink and F. A. Bilsen (Delft U. P., Delft, The Netherlands), pp. 7–14.

Kim, D. O., Molnar, C. E., and Matthews, J. W. (**1980b**). "Cochlear mechanics: Nonlinear behavior in two-tone responses as reflected in cochlear-nerve-fiber responses and in ear-canal sound pressure," J. Acoust. Soc. Am. **67**, 1704–1721.

Leonard, G., Smurzynski, J., Jung, M., and Kim, D. O. (**1990**). "Evaluation of distortion product otoacoustic emissions as a basis for the objective clinical assessment of cochlear function," in *Advances in Audiology* (Karger, Switzerland), Vol. 7, Chap. 13.

Matthews, J. W., and Molnar, C. E. (**1986**). "Modeling of intracochlear and ear canal distortion product $(2f_1 - f_2)$," in *Peripheral Auditory Mechanisms*, edited by J. B. Allen, J. L. Hall, A. Hubbard, S. T. Neely, and A. Tubis (Springer-Verlag, New York), pp. 258–265.

Neely, S. T., and Kim, D. O. (**1986**). "A model for active elements in cochlear biomechanics," J. Acoust. Soc. Am. **79**, 1472–1480.

Nelson, D. A., and Kimberley, B. P. (**1992**). "Distortion product emissions (DPEs) and auditory sensitivity in human ears with normal hearing and cochlear hearing loss," J. Speech Hear. Res. (in press).

Probst, R., Lonsbury-Martin, B. L., and Martin, G. K. (**1991**). "A review of otoacoustic emissions," J. Acoust. Soc. Am. **89**, 2027–2067.

Puria, S., and Allen, J. B. (**1991**). "Modeling the 'surgically modified' middle ear," in preparation.

Rhode, W. S. (**1971**). "Observations of the vibration of the basilar membrane in squirrel monkeys using the Mossbauer technique," J. Acoust. Soc. Am. **49**, 1218–1231.

Rhode, W. S. (**1978**). "Some observations on cochlear mechanics," J. Acoust. Soc. Am. **64**, 158–176.

Robles, L. A., Ruggero, M. A., and Rich, N. C. (**1986**). "Basilar membrane mechanics at the base of the chinchilla cochlea I. Input–output functions, tuning curves, and response phases," J. Acoust. Soc. Am. **80**, 1364–1374.

Sellick, P. M., Patuzzi, R., and Johnstone, B. M. (**1982**). "Measurement of basilar membrane motion in the guinea pig using the Mossbauer technique," J. Acoust. Soc. Am. **72**, 131–141.

Zweig, G. (**1991**). "Finding the impedance of the organ of Corti," J. Acoust. Soc. Am. **89**, 1229–1254.